

Up-to N^3LO heavy-baryon chiral perturbation theory calculation for the M1 properties of three-nucleon systems

Young-Ho Song*

Department of Physics, Duke University, Durham, NC 27708, USA

Rimantas Lazauskas†

*IPHC, IN2P3-CNRS/Université Louis Pasteur BP 28,
F-67037 Strasbourg Cedex 2, France*

Tae-Sun Park‡

*Department of Physics and BAERI,
Sungkyunkwan University, Suwon 440-746, Korea*

(Dated: November 14, 2018)

Abstract

M1 properties, comprising magnetic moments and radiative capture of thermal neutron observables, are studied in two- and three-nucleon systems. We utilize meson exchange current derived up to N^3LO using heavy baryon chiral perturbation theory a la Weinberg. Calculations have been performed for several qualitatively different realistic nuclear Hamiltonians, which permits us to analyze model dependence of our results. Our results are found to be strongly correlated with the effective range parameters such as binding energies and the scattering lengths. Taking into account such correlation, the results are in good agreement with the experimental data with small model-dependence.

PACS numbers: 21.45.+v,11.80.J,25.40.H,25.10.+s

*Electronic address: yhsong@phy.duke.edu

†Electronic address: rimantas.lazauskas@ires.in2p3.fr

‡Electronic address: tspark@kias.re.kr

I. INTRODUCTION

M1 properties – nuclear magnetic moments as well as radiative capture cross sections – are the fundamental low-energy observables of a few nucleon systems and therefore presents ideal laboratory to test effective field theories (EFTs). In this regard, M1 properties have been extensively studied using EFT with huge successes [1, 2, 3, 4, 5, 6, 7]. One such example is the ability to describe σ_{np} , the capture cross section of the $np \rightarrow d\gamma$ process, at threshold with 1 % accuracy by applying heavy-baryon chiral perturbation theory (HBChPT) up to next-next-next-to the leading order or N³LO [1]. In this work, we extend our up-to N³LO HBChPT description of the M1 properties to $A = 3$ systems. By taking the magnetic moments of ${}^3\text{H}$ and ${}^3\text{He}$ as input to fix the coefficients of the contact-term operators, a completely parameter-free theory predictions will be made for the total cross section and the photon polarization of the thermal neutron capture process ($nd \rightarrow {}^3\text{H}\gamma$). We will also revisit the theory predictions for the two-body observables: deuteron magnetic moment μ_d and σ_{np} .

The purpose of this article is to demonstrate the general tenet of EFTs by studying the M1 properties of a few body systems: once the long-range contributions are taken into account correctly, EFTs enables accurate and model-independent results, regardless the details of the short-range physics.

We begin with a few comments that are generic to all EFTs. At a certain order in EFTs, there appear contact-terms (CTs), which parameterize the high-energy (or short-range) physics above the cutoff scale of the theory. The coefficients of CTs – which we refer to as low-energy constants (LECs) – are thus sensitive to the short-range physics, and depend on the adopted cutoff value and the regularization/renormalization scheme. The values of LECs are not fixed by the symmetry alone, and should be determined by either solving the underlying theory or by fitting them so as to reproduce selected set of known experimental data. Since the former is currently not feasible, the latter remains the only practical option. At N³LO, HBChPT M1 currents contain two non-derivative two-nucleon CTs, one in iso-vector and the other in iso-scalar channel. These LECs, g_{4v} and g_{4s} , will be determined in this work by requiring to reproduce the experimental values of the magnetic moments of ${}^3\text{H}$ and ${}^3\text{He}$. Once these LECs fixed, we are left with no free parameters and can make

totally parameter-free theory predictions for the other M1 observables^{#1}. Note that the CT contributions have been ignored in Ref. [1], which caused small cutoff-dependence in σ_{np} . By taking into account of the LECs, we will show that σ_{np} becomes virtually completely cutoff-independent. Second comment is about the accuracy of the adopted wave functions at short range. The authors of Ref. [8] have developed an approach called EFT* or MEEFT (*more effective* effective field theory) that enables a consistent and systematic EFT calculations on top of accurate but phenomenological wave functions. The key observations are following. The model-dependence resides mainly in the short-range region of the wave functions. Since short-range contributions can be well embodied by local operators at low-energy and since EFT has the machinery to contain all the relevant local operators (i.e., CTs) in a consistent and systematic manner, the model-dependence due to short-range physics is to be absorbed into the renormalization procedure of the LECs. To be more specific, if we adopt other wave functions that have different short-range behavior, the values of LECs should also be changed so as to reproduce the selected experimental data *with* the adopted wave functions. By performing this procedure, while the values of LECs – which are not physical observables – are model-dependent, the resulting net contributions become model-independent. An easy and effective way of proving the model-independence in a quantitative fashion might be to look at the cutoff-dependence of the results, since the cutoff value is the key parameter that characterize the short-range contributions. Such a numerical proof will be taken in this work. The third comment is about the long-range contributions. Note that mismatches in the long-range contributions cannot be cured by finite set of local operators. The long-range part of the transition operator is usually governed by the chiral symmetry, leaving little uncertainty there. On the other hand, the long-range part of the wave functions is controlled by the effective range parameters (ERPs) such as the nuclear binding energies and the scattering lengths. For two-nucleon systems, most of the modern realistic NN potentials reproduce the ERPs with a great accuracy. However for nucleon systems with $A \geq 3$, situation becomes highly non-trivial as many of the available potentials fail to reproduce the relevant ERPs to the desired accuracy.

As we will demonstrate, our results have little cutoff-dependence for all the cases con-

^{#1} There are many other alternatives. For example, one can fix g_{4v} and g_{4s} from the experimental values of σ_{np} and the deuteron magnetic moment μ_d , and then make theory predictions on $\mu(^3\text{H})$ and $\mu(^3\text{He})$ [7].

sidered, which might be interpreted that the short-range physics is well under control. On the other hand, the model-dependence due to the difference in long-range part of the wave functions will cause correlations of the matrix elements with the ERPs. In our work, we observe rather a strong model-dependence and demonstrate how it is correlated to the model prediction of the triton binding energy B_3 . It indicates that the model-dependence is due to the mismatches in the long-range contributions.

To bypass the difficulty and to get model-independent accurate theory predictions, we have explored two different approaches. One is to bring prediction of B_3 to its experimental value $B_3^{\text{exp}} = 8.482$ MeV, using the observed correlation curves. The resulting M1 matrix elements are found to be model-independent to a good accuracy, and consistent with the experimental data. Another way is to adjust the tri-nucleon interactions (TNIs) to meet the experimental values of the ERPs.

II. FORMALISM

A. Faddeev equations

During the last few decades several different methods permitting to solve three body bound and scattering problem has been developed. In this study we solve Faddeev [9] equations (also often called Kowalski-Noyes equations) in configuration space to obtain 3-body bound and scattering wave functions. We employ the isospin formalism, i.e., consider proton and neutron as two degenerate states of the same particle - nucleon, having the mass fixed to $\hbar^2/m = 41.471$ MeV·fm. Then three Faddeev equations become formally identical, having the form

$$(E - H_0 - V_{ij}) \Phi_{ij,k} = V_{ij}(\Phi_{jk,i} + \Phi_{ki,j}), \quad (1)$$

where (ijk) are particle indices, H_0 is kinetic energy operator, V_{ij} is two body force between particles i and j , $\Phi_{ij,k}$ is Faddeev component. It is useful to define cyclic (P^+) and anti-cyclic (P^-) particle permutation operators, which permits to transform Faddeev component between two particle bases: $P^+ = (P^-)^{-1} = P_{23}P_{12}$ and $P^+\Phi_{ij,k} = \Phi_{jk,i}$, while $P^-\Phi_{ij,k} = \Phi_{ki,j}$. The wave function in Faddeev formalism is the sum of three Faddeev components, which employing permutation operators can be written as:

$$\Psi = (1 + P^+ + P^-)\Phi_{ij,k}. \quad (2)$$

Faddeev components, if represented in its proper coordinate basis, have simple structure and analytical asymptotic behavior for the short-range potentials. We use relative Jacobi coordinates $\mathbf{x}_k = (\mathbf{r}_j - \mathbf{r}_i)$ and $\mathbf{y}_k = \frac{2}{\sqrt{3}}(\mathbf{r}_k - \frac{\mathbf{r}_i + \mathbf{r}_j}{2})$, whereas Faddeev components we expand in bipolar harmonic basis:

$$\Phi_{ij,k} = \sum_{\alpha} \frac{F_{\alpha}(x_k, y_k)}{x_k y_k} \left| (l_x (s_i s_j)_{s_x})_{j_x} (l_y s_k)_{j_y} \right\rangle_{JM} \otimes \left| (t_i t_j)_{t_x} t_k \right\rangle_{TT_z}, \quad (3)$$

here index α represents all the symmetry allowed combinations of the quantum numbers presented in the brackets: l_x and l_y are the partial angular momenta associated with respective Jacobi coordinates; s_i and t_i are the spins and isospins of the individual particles. Functionals $F_{\alpha}(x_k, y_k)$ are called partial Faddeev amplitudes. Three-nucleon system conserves its total angular momentum J as well as its projection M , however due to the presence of charge dependent terms in nuclear interaction, total isospin of the system T is not conserved.

Equation (1) is not complete, it should be complemented with the appropriate boundary conditions. Boundary conditions can be written in the Dirichlet form. First Faddeev amplitudes, for bound as well as for scattering states, satisfy the regularity conditions:

$$F_{\alpha}(0, y_k) = F_{\alpha}(x_k, 0) = 0. \quad (4)$$

For the bound state problem wave function is compact, therefore the regularity conditions can be completed by forcing the amplitudes F_{α} to vanish at the borders of a hypercube $[0, X_{\max}] \times [0, Y_{\max}]$:

$$F_{\alpha}(X_{\max}, y_k) = F_{\alpha}(x_k, Y_{\max}) = 0. \quad (5)$$

Finally, we normalize three-nucleon wave function to unity $\langle \Psi | \Psi \rangle = 1$.

Faddeev components describing neutron-deuteron scattering, for the energies below the break-up threshold, vanish for $\mathbf{x}_k \rightarrow \infty$. As $\mathbf{y}_k \rightarrow \infty$ interaction between particle k and cluster ij is negligible and Faddeev components $\Phi_{jk,i}$ and $\Phi_{ki,j}$ vanish. Then the component $\Phi_{ij,k}$ describes the plane wave of the particle k with respect to the bound particle pair ij :

$$\begin{aligned} \lim_{y_k \rightarrow \infty} \Phi_{ij,k}(\mathbf{x}_k, \mathbf{y}_k) &= \frac{1}{\sqrt{3}} \sum_{j'_n l'_n} \left| \{ \psi_d(\mathbf{x}_k) \}_{j_d} \otimes \{ Y_{l_n}(\hat{\mathbf{y}}_k) \otimes s_k \}_{j_n} \right\rangle_{JM} \otimes \left| (t_i t_j)_{t_d} t_k \right\rangle_{\frac{1}{2}, -\frac{1}{2}} \\ &\times \frac{i}{2} \left[h_{l_n}^{-}(pr_{nd}) - S_{j_n l_n, j'_n l'_n} h_{l_n}^{+}(pr_{nd}) \right], \end{aligned} \quad (6)$$

where deuteron, being formed from nucleons i and j , has quantum numbers $s_d = 1$, $j_d = 1$ and $t_d = 0$ and its wave function $\psi_d(\mathbf{x}_k)$ is normalized to unity; p designates the relative

momentum of incoming neutron, $r_{nd} = (\sqrt{3}/2)y_k$ is relative distance between neutron and deuteron target, whereas $h_{l_n}^\pm$ are the spherical Hankel functions. Expression (6) is normalized so that nd scattering wave function has unity flux.

For zero or very low momentum neutrons, as is the case for the thermal neutron capture, only relative S -wave amplitudes survives in the asymptote, whereas expression (6) simplifies to:

$$\lim_{y_k \rightarrow \infty} \Phi_{ij,k}(\mathbf{x}_k, \mathbf{y}_k) = \frac{1}{\sqrt{3}} \sum_{j'_n l'_n} \left| \{ \psi_d(\mathbf{x}_k) \}_{j_d} \otimes \{ Y_{l_n}(\hat{\mathbf{y}}_k) \otimes s_k \}_{j_n} \right\rangle_{JM} \otimes \left| (t_i t_j)_{t_d} t_k \right\rangle_{\frac{1}{2}, -\frac{1}{2}} \times \left[1 - \frac{2^{J+1} a_{nd}}{r_{nd}} \right], \quad (7)$$

where $2^{J+1} a_{nd}$ is neutron-deuteron scattering length. For the cases where Urbana type three-nucleon interaction (TNI) are included, noting that the TNI among particles ijk can be written as sum of three terms $V_{ijk} = V_{ij}^k + V_{jk}^i + V_{ki}^j$, we modify the Faddeev equation (1) into:

$$(E - H_0 - V_{ij}) \Phi_{ij,k} = V_{ij}(P^+ + P^-) \Phi_{ij,k} + \frac{1}{2}(V_{jk}^i + V_{ki}^j) \Psi. \quad (8)$$

B. Electromagnetic current

For three-body system one has three 1-body currents associated with each particle and three 2-body currents associated with each pair of particles. Thus

$$J_{em} = \sum_{i=1, i \neq (j < k)}^3 (J_{1B}^{(i)} + J_{2B}^{(jk)}). \quad (9)$$

Since the wave-functions $|\Psi\rangle$ in isospin formalism is fully antisymmetric, the matrix element of the current operators can be written as

$$\langle \Psi_f | J_{em} | \Psi_i \rangle = \sum_{i=1, i \neq (j < k)}^3 \langle \Psi_f | J_{1B}^{(i)} + J_{2B}^{(jk)} | \Psi_i \rangle = 3 \langle \Psi_f | J_{1B}^{(3)} | \Psi_i \rangle + 3 \langle \Psi_f | J_{2B}^{(12)} | \Psi_i \rangle, \quad (10)$$

We use the electromagnetic current operators derived from HBchPT, which contain the nucleons and pions as pertinent degrees of freedom with all other massive fields integrated out. In HBchPT the electromagnetic currents and M1 operator are expanded systematically with increasing powers of Q/Λ_χ , where Q stands for the typical momentum scale of the process and/or the pion mass, and $\Lambda_\chi \sim 4\pi f_\pi \sim m \sim 1$ GeV is the chiral scale, $f_\pi \sim 92.4$

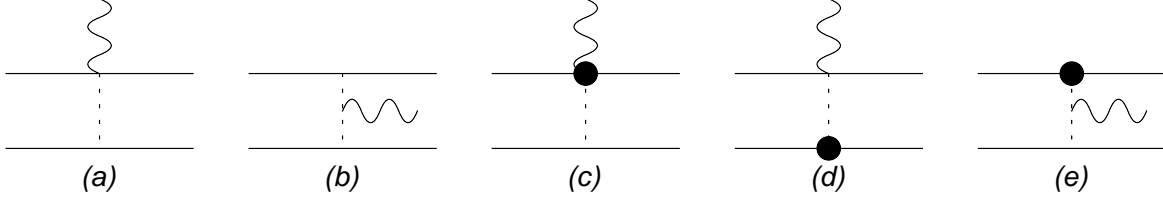


FIG. 1: Tree diagrams for the electromagnetic current operators. Soft one-pion-exchange, the sum of the “seagull” (a) and the “pion-pole” (b) diagrams contribute to the $J_{1\pi}$. Diagrams (c) – (e) contribute to the $J_{1\pi C}$ at N³LO. The dot represents the vertex corrections coming from NLO or N²LO lagrangian.

MeV is the pion decay constant, and m is the nucleon mass. We remark that, while the nucleon momentum \mathbf{p} is of order of Q , its energy ($\sim \frac{\mathbf{p}^2}{m}$) is of order of Q^2/m , and consequently the four-momentum of the emitted photon $q^\mu = (\omega, \mathbf{q})$ with $|\mathbf{q}| = \omega$ also is counted as $O(Q^2/m)$. Current operators are obtained up to N³LO. Note that three-body currents are N⁴LO or higher order, and do not enter in our work. #2

Let us list the relevant current operators. The explicit form of magnetic moment operators can be found in the ref. [7]. The one-body current including the relativistic corrections reads

$$\begin{aligned}
J_{1B}^{(i)}(\mathbf{q}; \mathbf{r}_i) = e^{-i\mathbf{q}\cdot\mathbf{r}_i} & \left[\frac{Q_i}{m} \bar{\mathbf{p}}_i \left(1 - \frac{\bar{\mathbf{p}}_i^2}{2m} \right) + \frac{1}{2m} i\mathbf{q} \times \boldsymbol{\sigma}_i \left(\mu_i - \frac{Q_i}{2m^2} \bar{\mathbf{p}}_i^2 \right) \right. \\
& - \frac{\omega(2\mu_i - Q_i)}{8m^2} (2i\bar{\mathbf{p}}_i \times \boldsymbol{\sigma}_i) - \frac{\mu_i - Q_i}{16m^3} (4i\mathbf{q} \times \bar{\mathbf{p}}_i \boldsymbol{\sigma}_i \cdot \bar{\mathbf{p}}_i) \\
& \left. - \frac{\omega(2\mu_i - Q_i)}{8m^2} \mathbf{q} - \frac{\mu_i - Q_i}{16m^3} (-2\mathbf{q}\mathbf{q} \cdot \bar{\mathbf{p}}_i) + (\text{higher orders}) \right] \quad (11)
\end{aligned}$$

where Q_i and μ_i represent the charge and magnetic moment of i -th nucleon, and $\bar{\mathbf{p}} \equiv \frac{1}{2}(i \overleftarrow{\nabla} - i \overrightarrow{\nabla})$ should be understood to act only on the nuclear wave functions.

Corrections to the 1B operator are due to the meson-exchange currents (MECs). Up to N³LO, as mentioned, only two-body (2B) contributions enter. It is to be emphasized that MECs derived in EFT are meaningful only up to a certain momentum scale characterized by the cutoff Λ . In our work, we adopt a Gaussian regulator in performing the Fourier

#2 It is worth mentioning that there is a different power counting scheme where the nucleon mass is regarded as heavier than the chiral scale, $m \sim \Lambda_\chi^2/Q$, see refs. [10, 11] for details. However, the use of this alternative counting scheme would not affect the results to be reported in this work since the difference between the two counting schemes would appear only at higher orders than explicitly considered here (N³LO).

transformation of the MECs from momentum space to coordinate space [8]. It is to be noted that the contributions due to high momentum exchanges (above the cutoff scale) are not simply ignored but, as we will discuss later, they are accounted for by the renormalization of the contact-term coefficients.

We decompose the two-body current into the soft-one-pion-exchange (1π), vertex corrections to the one-pion exchange ($1\pi C$), the two-pion-exchanges (2π), and the contact-term (CT) contributions,

$$J_{2B}^{(jk)} = J_{1\pi}^{(jk)} + J_{1\pi C}^{(jk)} + J_{2\pi}^{(jk)} + J_{CT}^{(jk)}. \quad (12)$$

It is noteworthy that there can be additional corrections to the 2-body current coming from the so-called fixed term. The fixed-term contributions represent vertex corrections to the soft-one-pion-exchange and fixed completely by Lorentz covariance. Because the fixed terms make the calculation highly involved, but only give very small contributions in M1 operator according to our previous study [7], we neglected the fixed term contributions in the present work.

The soft-one-pion exchange current $J_{1\pi}^{(jk)}$ is NLO and can be written in terms of $\mathbf{R}_{jk} = \frac{1}{2}(\mathbf{r}_j + \mathbf{r}_k)$, $\mathbf{r} = \mathbf{r}_j - \mathbf{r}_k$, $\hat{\mathbf{r}} = \mathbf{r}/|\mathbf{r}|$, $S_{jk} = 3\boldsymbol{\sigma}_j \cdot \hat{\mathbf{r}} \boldsymbol{\sigma}_k \cdot \hat{\mathbf{r}} - \boldsymbol{\sigma}_j \cdot \boldsymbol{\sigma}_k$,

$$J_{1\pi}^{(jk)}(\mathbf{r}, \mathbf{R}) = e^{-i\mathbf{q}\cdot\mathbf{R}} \left\{ -\frac{g_A^2 m_\pi^2}{12f_\pi^2} (\vec{\tau}_j \times \vec{\tau}_k)^z \boldsymbol{\tau} \left[\vec{\sigma}_j \cdot \vec{\sigma}_k \left(y_{0\Lambda}^\pi(r) - \frac{\delta_\Lambda(r)}{m_\pi^2} \right) + S_{jk} y_{2\Lambda}^\pi(r) \right] \right. \\ \left. + i \frac{g_A^2}{8f_\pi^2} \mathbf{q} \times \left[\hat{T}_{S,jk}^{(\times)} \left(\frac{2}{3} y_{1\Lambda}^\pi(r) - y_{0\Lambda}^\pi(r) \right) - \hat{T}_{T,jk}^{(\times)} y_{1\Lambda}^\pi(r) \right] \right\},$$

where

$$\hat{T}_{S,jk}^{(\odot)} = (\tau_j \odot \tau_k)^z (\boldsymbol{\sigma}_j \odot \boldsymbol{\sigma}_k), \\ \hat{T}_{T,jk}^{(\odot)} = (\tau_j \odot \tau_k)^z \left[\hat{\mathbf{r}} \hat{\mathbf{r}} \cdot (\boldsymbol{\sigma}_j \odot \boldsymbol{\sigma}_k) - \frac{1}{3} (\boldsymbol{\sigma}_j \odot \boldsymbol{\sigma}_k) \right], \quad (13)$$

$\odot = \pm, \times$, and the regulated delta and Yukawa functions are defined as

$$\delta_\Lambda(r) \equiv \int \frac{d^3\mathbf{k}}{(2\pi)^3} e^{-k^2/\Lambda^2} e^{i\mathbf{k}\cdot\mathbf{r}} \\ y_{0\Lambda}^\pi(r) \equiv \int \frac{d^3\mathbf{k}}{(2\pi)^3} e^{-k^2/\Lambda^2} e^{i\mathbf{k}\cdot\mathbf{r}} \frac{1}{\mathbf{k}^2 + m_\pi^2} \\ y_{1\Lambda}^\pi(r) \equiv -r \frac{\partial}{\partial r} y_{0\Lambda}^\pi(r), \quad y_{2\Lambda}^\pi(r) \equiv \frac{r}{m_\pi^2} \frac{\partial}{\partial r} \frac{1}{r} \frac{\partial}{\partial r} y_{0\Lambda}^\pi(r). \quad (14)$$

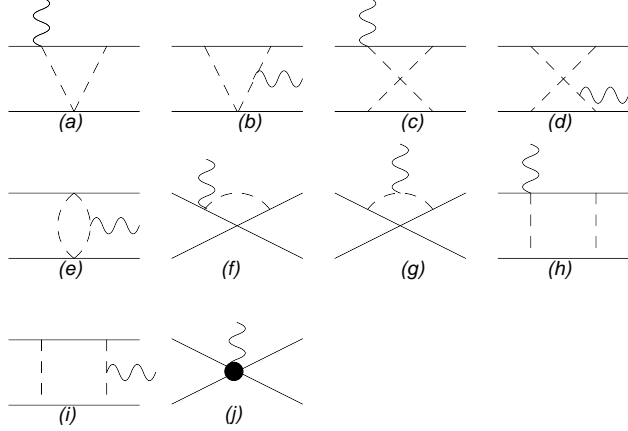


FIG. 2: Diagrams which contribute to $J_{2\pi}$ (a)-(i) and J_{CT} (j) at N³LO.

The one-loop vertex correction to the one-pion exchange has been investigated in detail in refs. [1, 2],

$$\begin{aligned}
J_{1\pi C}^{(12)} = e^{-i\mathbf{q}\cdot\mathbf{R}} i\mathbf{q} \times \left\{ -\frac{g_A^2}{8f_\pi^2} (\bar{c}_\omega + \bar{c}_\Delta) [(\hat{T}_S^{(+)} + \hat{T}_S^{(-)}) \frac{\bar{y}_{0\Lambda}^\pi}{3} + (\hat{T}_T^{(+)} + \hat{T}_T^{(-)}) y_{2\Lambda}^\pi] \right. \\
\left. + \frac{g_A^2}{8f_\pi^2} \bar{c}_\Delta [\frac{1}{3} \hat{T}_S^{(\times)} \bar{y}_{0\Lambda}^\pi - \frac{1}{2} \hat{T}_T^{(\times)} y_{2\Lambda}^\pi] \right. \\
\left. - \frac{1}{16f_\pi^2} \bar{N}_{WZ} \boldsymbol{\tau}_1 \cdot \boldsymbol{\tau}_2 [(\boldsymbol{\sigma}_1 + \boldsymbol{\sigma}_2) \bar{y}_{0\Lambda}^\pi + (3\hat{r}\hat{r} \cdot (\boldsymbol{\sigma}_1 + \boldsymbol{\sigma}_2) - (\boldsymbol{\sigma}_1 + \boldsymbol{\sigma}_2)) y_{2\Lambda}^\pi] \right\}, \quad (15)
\end{aligned}$$

The values of the LECs (\bar{c}_ω , \bar{c}_Δ , \bar{N}_{WZ}) should in principle be fixed either by solving the underlying theory, QCD, or by fitting to suitable experimental observables. Since this has not yet been done, we adopt here the estimates given in refs. [1, 2] based on the resonance saturation assumption and the Wess-Zumino action, $(\bar{c}_\omega, \bar{c}_\Delta, \bar{N}_{WZ}) \simeq (0.1021, 0.1667, 0.02395)$.

The two-pion exchange diagrams give rise to

$$J_{2\pi}^{jk} = \frac{e^{-i\mathbf{q}\cdot\mathbf{R}}}{128\pi^2 f_\pi^4} \left(i\mathbf{q} \times [(\hat{T}_S^{(+)} - \hat{T}_S^{(-)}) L_S(r) + (\hat{T}_T^{(+)} - \hat{T}_T^{(-)}) L_T(r)] - (\tau_j \times \tau_k)^z \hat{r} \frac{d}{dr} L_0(r) \right) \quad (16)$$

where

$$\begin{aligned}
L_S(r) &= -\frac{g_A^2}{3} r \frac{d}{dr} K_0 + \frac{g_A^4}{3} (-2K_0 + 4K_1 + r \frac{d}{dr} K_0 + 2r \frac{d}{dr} K_1) \\
L_T(r) &= \frac{g_A^2}{2} r \frac{d}{dr} K_0 + \frac{g_A^4}{2} (4K_T - r \frac{d}{dr} K_0 - 2r \frac{d}{dr} K_1) \\
L_0(r) &= 2K_2 + g_A^2 (8K_2 + 2K_1 + 2K_0) - g_A^4 (16K_2 + 5K_1 + 5K_0) + g_A^4 \frac{d}{dr} (rK_1), \quad (17)
\end{aligned}$$

and the loop functions K 's are defined in refs. [1, 8].

Finally, contact-term contributions have the form

$$J_{CT}^{(jk)} = e^{-i\mathbf{q}\cdot\mathbf{R}} \frac{i}{2m_p} \mathbf{q} \times [g_{4S}(\boldsymbol{\sigma}_j + \boldsymbol{\sigma}_k) + g_{4V}T_S^{(\times)}] \delta_\Lambda(r) \quad (18)$$

where $g_{4S} = m_p g_4$ and $g_{4V} = -m_p(G_A^R + \frac{1}{4}E_T^{V,R})$. We remark that, three contact terms were introduced in refs. [1, 2], whose coefficients are denoted as g_4 , G_A^R and $E_T^{V,R}$. However, due to Fermi-Dirac statistics, only two of them are independent, and consistent with Eq. (18). A similar reduction has been noticed for the Gamow-Teller operator, where only one linear combination of two CTs is required [8].

C. n - d radiative capture

In center of mass frame, each currents can be written in the form of

$$J_{em} = e^{-i\mathbf{q}\cdot\mathbf{x}} (i\mathbf{q} \times \mathbf{j}_\mu + \mathbf{j}_c) \quad (19)$$

where \mathbf{x} is \mathbf{r}_i for $J_{1B}^{(i)}$ and \mathbf{R}_{jk} for $J_{2B}^{(jk)}$.

To calculate neutron radiative capture observables we will use multipole expansion. First we introduce a shorthand notations for the multipoles:

$$\begin{aligned} F_{JM}(\hat{\mathbf{r}}) &= j_J(qr) Y_{JM}(\hat{\mathbf{r}}), \\ F_{JL}^M(\hat{\mathbf{r}}) &= j_L(qr) \mathcal{Y}_{JL1}^M(\hat{\mathbf{r}}), \end{aligned} \quad (20)$$

where $j_L(qr)$ is the spherical Bessel function; Y_{JM} and \mathcal{Y}_{JL1}^M are spherical and vector-spherical harmonics respectively; r is a vector describing the particle (nucleon or meson), which interacts with EM field. Then the electric and magnetic multipoles read

$$\begin{aligned} \mathcal{M}_{JM} &= F_{JJ}^M(\hat{\mathbf{r}}) \cdot \mathbf{j}_c + iq \left[\left(\frac{J+1}{2J+1} \right)^{1/2} F_{JJ-1}^M(\hat{\mathbf{r}}) - \left(\frac{J}{2J+1} \right)^{1/2} F_{JJ+1}^M(\hat{\mathbf{r}}) \right] \cdot \mathbf{j}_\mu, \\ \mathcal{E}_{JM} &= i \left[\left(\frac{J+1}{2J+1} \right)^{1/2} F_{JJ-1}^M(\hat{\mathbf{r}}) - \left(\frac{J}{2J+1} \right)^{1/2} F_{JJ+1}^M(\hat{\mathbf{r}}) \right] \cdot \mathbf{j}_c + q F_{JJ}^M(\hat{\mathbf{r}}) \cdot \mathbf{j}_\mu. \end{aligned} \quad (21)$$

With the explicit expressions of the $F_{1L}^M(\hat{\mathbf{r}})$, M1 multipoles can also be written as

$$\mathcal{M}_{1M} = i \sqrt{\frac{3}{8\pi}} j_1(qr) [\hat{\mathbf{r}} \times \mathbf{j}_c] + \frac{iq}{\sqrt{6\pi}} \left[j_0(qr) \mathbf{j}_\mu - \frac{1}{2} j_2(qr) \{ \mathbf{j}_\mu - \hat{\mathbf{r}} (\hat{\mathbf{r}} \cdot \mathbf{j}_\mu) \} \right]. \quad (22)$$

In terms of the reduced matrix elements (RMEs) [12, 13],

$$\tilde{\mathcal{X}}_J^{J_i J_f} = \frac{\sqrt{6\pi}}{q\mu_N} \sqrt{4\pi} \langle \Psi_{b.s.}^{J_f} \| \mathcal{X}_{JM} \| \Psi_{scat}^{J_i} \rangle, \quad (23)$$

where $\mathcal{X}_{JM} = (\mathcal{M}_{JM}, \mathcal{E}_{JM})$, the total nd capture cross section is given by

$$\sigma_{nd} = \frac{2}{9} \frac{\alpha}{(v_{rel}/c)} \left(\frac{\hbar c}{2mc^2} \right)^2 \left(\frac{q}{\hbar c} \right)^3 \sum_{J_i} \sum_{J=1}^{J_i+\frac{1}{2}} \left(\left| \widetilde{\mathcal{E}}_J^{J_i, \frac{1}{2}} \right|^2 + \left| \widetilde{\mathcal{M}}_J^{J_i, \frac{1}{2}} \right|^2 \right). \quad (24)$$

Thermal neutron capture proceeds only from doublet $J_i^\Pi = \frac{1}{2}^+$ and quartet $J_i^\Pi = \frac{3}{2}^+$ nd scattering states, since only these two states comprise nd S -wave asymptote and thus dominate low energy scattering. Since final state (the triton) is $J_f^\Pi = \frac{1}{2}^+$, therefore only magnetic dipole transition elements $m_2 \equiv \widetilde{\mathcal{M}}_1^{\frac{1}{2}, \frac{1}{2}}$, $m_4 \equiv \widetilde{\mathcal{M}}_1^{\frac{3}{2}, \frac{1}{2}}$ and electric quadrupole transition element $e_4 \equiv \widetilde{\mathcal{E}}_2^{\frac{3}{2}, \frac{1}{2}}$ do not vanish. Notice that magnetic dipole moments are purely imaginary, while electric quadrupole moment is real.

Experimentally, in addition to capture cross section, photon polarization parameter R_c can also be measured. This parameter is given by [13]

$$R_c = \frac{1}{3} \left[\frac{\frac{7}{2} |m_4|^2 + \sqrt{8} \text{Re} [m_2 m_4^*] + \frac{5}{2} |e_4|^2 + \sqrt{24} \text{Im} [m_2 e_4^*] - \sqrt{3} \text{Im} [m_4 e_4^*]}{|m_2|^2 + |m_4|^2 + |e_4|^2} - 1 \right]. \quad (25)$$

Calculations using expression (10) are numerically stable for all the two- and one-body current terms except the ones entering into impulse approximation of M1 operator. This issue has been observed and the special numerical procedure developed in reference [14], we have successfully followed it.

III. RESULTS

A. Binding energies and scattering lengths

In this work we have performed rigorous calculations for several qualitatively different realistic nuclear Hamiltonians, which are based on NN potentials defined both in configuration and momentum spaces. Argonne Av18 [15] is an accurate local NN potential in configuration space. Semi-realistic configuration space potential INOY has been recently derived by Doleschall [16], which can describe binding energies of three-nucleon systems with only two-nucleon forces. ISUJ [17]— a recent revision of INOY — further improves description of np and pp data and at low energies provides solution for the long standing “Ay puzzle” of N - d scattering. We have also tested some chiral N³LO potentials defined in momentum space: Idaho group potential [18] (referred to as I-N3LO), and three different parameterizations of chiral N³LO potential of Bonn-Bochum group [10]. In particular Bonn-Bochum

TABLE I: Values for np singlet scattering length and deuteron binding energy obtained using Bonn-Bochum group potentials.

| Model | $^1a_{np}$ (fm) | B_{H_2} (MeV) |
|---------|-----------------|-----------------|
| B1-N3LO | -23.60 | 2.215 |
| B2-N3LO | -23.72 | 2.218 |
| B3-N3LO | -23.64 | 2.220 |
| Exp.: | -23.74 | 2.225 |

group potentials parameterized with set of cut-off values $\{\Lambda, \tilde{\Lambda}\} = \{450, 500\}, \{450, 700\}$ and $\{600, 700\}$ MeV have been used and are referred to as B1-N3LO, B2-N3LO and B3-N3LO respectively.

All the NN potentials mentioned above describe the NN data quite accurately. And all but Bonn-Bochum group potentials reproduce experimental deuteron binding energy B_d and the singlet np scattering length $^1a_{np}$ with at least four significant digit accuracy. Values of these observables obtained using Bonn-Bochum group potentials are summarized in Table I.

Our three-body calculations have been carried out considering isospin breaking effects, which allow admixture of total isospin $T = 3/2$ in the wave functions. The Argonne UIX three-nucleon interaction [19] also has been taken into account in the combination with Av18 NN potential.

The relevant properties of three-body systems obtained with the adopted models are summarized in Table II. These values are in perfect agreement with ones obtained by the other groups [16],[21]-[24]. In [25] we have already published three-nucleon properties for INOY and Av18 models, the small difference in fourth digit of those results compared with current ones is due to the small admixture of isospin $T = 3/2$ states. One should note that only INOY, ISUJ and Av18+UIX models reproduce experimental three-nucleon binding energies as well as neutron-deuteron doublet ($J = \frac{1}{2}$) scattering length accurately. Chiral potentials at N³LO comprise already two irreducible three-nucleon interaction diagrams with contact terms. The strength of these contact terms may be *a priori* adjusted so as to reproduce three-nucleon binding energy and scattering length [26]. In this work however only two-nucleon interaction part of N³LO models was considered.

TABLE II: Three-nucleon properties as calculated with different realistic Hamiltonians. They contain: nd doublet (${}^2a_{nd}$) and quartet (${}^4a_{nd}$) scattering lengths in fm; bound state properties comprising binding energy(BE), average kinetic energy ($\langle T \rangle$) in MeV's and rms radius $r_{\text{rms}} = \sqrt{\langle r^2 \rangle}$ in fm. These values are compared to other theoretical calculations and experimental results.

| Hamiltonian | Ref. | nd | | ${}^3\text{H}$ | | | ${}^3\text{He}$ | | |
|-------------|-----------|----------------------|----------------------|----------------|---------------------|------------------|-----------------|---------------------|------------------|
| | | ${}^2a_{nd}$ | ${}^4a_{nd}$ | BE | $\langle T \rangle$ | r_{rms} | BE | $\langle T \rangle$ | r_{rms} |
| Av18 | this work | 1.266 | 6.331 | 7.623 | 46.71 | 1.769 | 6.925 | 45.67 | 1.810 |
| | [21, 22] | 1.248 | 6.346 | 7.623(2) | | | 6.924(1) | | |
| AV18+UIX | this work | 0.598 | 6.331 | 8.483 | 51.29 | 1.683 | 7.753 | 50.23 | 1.716 |
| | [21, 22] | 0.578 | 6.347 | 8.478(2) | | | 7.748(2) | | |
| INOY | this work | 0.551 | 6.331 | 8.483 | 33.00 | 1.666 | 7.720 | 32.22 | 1.704 |
| | [16] | | | 8.482 | | | 7.718 | | |
| ISUJ | this work | 0.523 | 6.330 | 8.484 | 32.95 | 1.667 | | | |
| | [17] | | | 8.482 | | | 7.718 | | |
| I-N3LO | this work | 1.101 | 6.337 | 7.852 | 34.54 | 1.760 | 7.159 | 33.83 | 1.797 |
| | [23] | | | 7.854 | | | | | |
| B1-N3LO | this work | 1.263 | 6.334 | 7.636 | 33.60 | 1.816 | 6.904 | 32.79 | 1.860 |
| | [24] | | | 7.64 | | | | | |
| B2-N3LO | this work | 1.024 | 6.339 | 7.930 | 31.70 | 1.777 | 7.210 | 31.01 | 1.815 |
| | [24] | | | 7.97 | | | | | |
| B3-N3LO | this work | 1.781 | 6.329 | 7.079 | 47.25 | 1.863 | 6.403 | 46.17 | 1.909 |
| | [24] | | | 7.09 | | | | | |
| Exp: | | 0.65 ± 0.04 [20] | 6.35 ± 0.02 [20] | 8.482 | - | | 7.718 | - | |

B. Magnetic moments and thermal neutron capture

In Table III, we present M1 RMEs obtained for INOY Hamiltonian with $\Lambda=700$ MeV, listing the contributions from each chiral order. Note that the one-body contribution of the iso-scalar M1 RME, m_2 , is strongly suppressed due to the pseudo-orthogonality between initial and final wave functions. The chiral convergence is however not much illuminating, *i.e.*, N³LO contributions appear about the same size of NLO. This behavior is mainly due

TABLE III: Matrix elements calculated for magnetic moments and thermal neutron capture. These results are obtained using INOY Hamiltonian with $\Lambda=700$ MeV.

| | $\mu(^2\text{H})$ | $\mu(^3\text{H})$ | $\mu(^3\text{He})$ | $\frac{1}{i}\widetilde{\mathcal{M}}_1^{0,1}$ | $\frac{1}{i}\widetilde{\mathcal{M}}_1^{\frac{1}{2},\frac{1}{2}}$ | $\frac{1}{i}\widetilde{\mathcal{M}}_1^{\frac{3}{2},\frac{1}{2}}$ | $\widetilde{\mathcal{E}}_2^{\frac{3}{2},\frac{1}{2}}$ |
|-----------------------------|-------------------|-------------------|--------------------|--|--|--|---|
| LO: 1B | 0.8593 | 2.6567 | -1.8100 | 395.5000 | -13.6196 | 13.1149 | -0.0741 |
| N ³ LO: 1B | -0.0057 | -0.0199 | 0.0080 | -0.1653 | 0.4106 | 0.1048 | 0.0032 |
| NLO: 1π | 0.0000 | 0.1515 | -0.1501 | 7.0970 | -2.5712 | -0.4289 | 0.1562 |
| N ³ LO: $1\pi C$ | -0.0029 | 0.0839 | -0.0926 | 3.1860 | -2.7674 | -0.3465 | 0.0000 |
| N ³ LO: 2π | 0.0000 | 0.0374 | -0.0362 | 1.1290 | -1.2504 | -0.1223 | -0.0019 |
| g_{4S} | 0.0338 | 0.0457 | 0.0449 | 0.0000 | -0.9855 | 0.2647 | 0.0000 |
| g_{4V} | 0.0000 | 0.0733 | -0.0712 | 2.3130 | -2.5179 | -0.2267 | 0.0000 |

TABLE IV: Values of contact term coefficients g_{4s} and g_{4V} , which are obtained by fitting magnetic moments of triton and ^3He , for INOY Hamiltonian.

| Λ (MeV) | g_{4s} | g_{4V} |
|-----------------|----------|----------|
| 500 | 0.2747 | 1.8746 |
| 700 | 0.2313 | 0.8021 |
| 900 | 0.1997 | 0.4613 |

to the accidental cancelation between two NLO contributions, the seagull and pion-pole diagrams [30].

As explained, M1 currents contain two non-derivative contact-terms at N³LO. Since the coefficients of them, g_{4S} and g_{4V} , cannot be determined from the underlying theory yet, we fit these constants by requiring that magnetic moments of ^3H and ^3He are correctly reproduced. The resulting values obtained with INOY potential are given in Table IV. We remark that g_{4S} and g_{4V} depend on cutoff Λ as well as on particular choice of nuclear Hamiltonian.

Table V shows the cutoff dependence of our results. One-body contributions are cutoff independent by their construction. NLO results bring sizable cutoff-dependence, indicating that some important pieces are omitted at this level. As is indicated in the table, going N³LO but without taking the CTs does not help in resolving the situation. It is only after

TABLE V: Dependence of M1 observables for two and three-nucleon systems on cutoff value Λ . These results are obtained using INOY Hamiltonian.

| LO | | | | | | |
|--|-------------------|-------------------|--------------------|--------------------|--------------------|--------------------|
| Λ (MeV) | $\mu(^2\text{H})$ | $\mu(^3\text{H})$ | $\mu(^3\text{He})$ | σ_{np} (mb) | σ_{nd} (mb) | R_c |
| - | 0.8593 | 2.657 | -1.810 | 309.7 | 0.2785 | -0.2369 |
| NLO | | | | | | |
| Λ (MeV) | $\mu(^2\text{H})$ | $\mu(^3\text{H})$ | $\mu(^3\text{He})$ | σ_{np} (mb) | σ_{nd} (mb) | R_c |
| 500 | 0.8593 | 2.760 | -1.913 | 318.7 | 0.2972 | -0.3026 |
| 700 | 0.8593 | 2.808 | -1.960 | 320.9 | 0.3296 | -0.3538 |
| 900 | 0.8593 | 2.829 | -1.980 | 321.9 | 0.3480 | -0.3753 |
| N ³ LO without contact term | | | | | | |
| Λ (MeV) | $\mu(^2\text{H})$ | $\mu(^3\text{H})$ | $\mu(^3\text{He})$ | σ_{np} (mb) | σ_{nd} (mb) | R_c |
| 500 | 0.8499 | 2.836 | -2.011 | 324.1 | 0.3612 | -0.3896 |
| 700 | 0.8507 | 2.910 | -2.081 | 327.5 | 0.4237 | -0.4366 |
| 900 | 0.8515 | 2.937 | -2.105 | 328.8 | 0.4526 | -0.4504 |
| N ³ LO | | | | | | |
| Λ (MeV) | $\mu(^2\text{H})$ | $\mu(^3\text{H})$ | $\mu(^3\text{He})$ | σ_{np} (mb) | σ_{nd} (mb) | R_c |
| 500 | 0.8584 | 2.9790 | -2.1276 | 330.9 | 0.5012 | -0.4659 |
| 700 | 0.8585 | 2.9790 | -2.1276 | 330.5 | 0.4946 | -0.4649 |
| 900 | 0.8583 | 2.9790 | -2.1276 | 330.4 | 0.4959 | -0.4650 |
| Exp.: | 0.8574 | 2.9790 | -2.1276 | 332.6 \pm 0.7 | 0.508 \pm 0.015 | -0.420 \pm 0.030 |

the CTs taken into account that the results become almost independent of the cutoff, which implies that the CTs are quite effective in renormalizing away the details residing in the short-range region.

Results with varying model Hamiltonian are given in Table VI, with some relevant low-energy properties of the potentials. From the table, one observes that $\mu(^2\text{H})$ and σ_{np} are rather insensitive, R_c is moderately sensitive and the nd capture cross section, σ_{nd} , is highly sensitive on the model Hamiltonian. To understand the sensitivity, let us consider the model-dependence of the effective-range parameters (ERPs), which govern the long-range

part of the RMEs. The most important ERPs are the binding energies and the scattering lengths, which should strongly influence M1 RMEs through the coupling of the long-range parts of the three-nucleon wave functions. And indeed, as shown in Fig. 3, the M1 RMEs are strongly correlated with the triton binding energy B_3 . The correlation is found to be almost perfect for m_4 , while with some fluctuation for m_2 . These behavior can be explained with simple arguments: let us first concentrate on the quartet RME, m_4 . In spin-quartet states, Pauli principle inhibits three nucleons from gathering altogether, and thus observables are insensitive to short-range part of three-nucleon interaction. As a result, the nd quartet

TABLE VI: Predictions for the deuterons magnetic moment and the observables of the thermal neutron capture on protons and deuterons. These calculations have been realized by fixing contact terms of the meson exchange current in order to reproduce magnetic moments of the triton and ${}^3\text{He}$. These values turns to be insensitive to the cut-off parameter in the interval $\Lambda = (500, 900)$ MeV; if however variation was larger than one affecting the fourth significant digit it is given in parentheses. The constructed AV18+UIX* model gives ${}^2a_{nd}=0.623$ fm, ${}^4a_{nd}=6.331$ fm and $\text{BE}({}^3\text{He})=7.718$ MeV; the I-N3LO+UIX** results are ${}^2a_{nd}=0.634$ fm, ${}^4a_{nd}=6.339$ fm and $\text{BE}({}^3\text{He})=7.737$ MeV. Both these models are adjusted to reproduce experimental triton binding energy of $\text{BE}({}^3\text{H})=8.482$ MeV

| Model | $\mu({}^2\text{H})$ | σ_{np} (mb) | σ_{nd} (mb) | R_c |
|--------------|---------------------|----------------------|------------------------|-------------------------|
| AV18 | 0.8575 | 331.9(1) | 0.680(3) | -0.435 |
| AV18+UIX | 0.8604 | 330.6(2) | 0.478(3) | -0.458 |
| INOY | 0.8585 | 330.6(2) | 0.498(3) | -0.465 |
| ISUJ | 0.8585 | 331.1(2) | 0.501(2) | -0.466 |
| I-N3LO | 0.8574 | 330.4(3) | 0.626(2) | -0.441 |
| B1-N3LO | 0.8577 | 328.7(6) | 0.688(4) | -0.438(1) |
| B2-N3LO | 0.8588 | 331.0(4) | 0.609(4) | -0.448(1) |
| B3-N3LO | 0.8549 | 330.9(7) | 0.879(8) | -0.411(2) |
| AV18+UIX* | 0.8614(1) | 330.9(3) | 0.476(2) | -0.457(1) |
| I-N3LO+UIX** | 0.8590(1) | 329.7(3) | 0.477(3) | -0.468(1) |
| Exp.: | 0.8574 | 332.6 ± 0.7 [27] | 0.508 ± 0.015 [28] | -0.420 ± 0.030 [29] |

scattering length ${}^4a_{nd}$ has little model-dependence; all the models considered here reproduce ${}^4a_{nd}$ in excellent agreement with the experimental data. This explains the perfect correlation of m_4 with B_3 . On the contrary, spin-doublet states are free from the exclusion principle and sensitive to the short-range three-nucleon interaction. This makes the scattering length ${}^2a_{nd}$ largely model-dependent, see Table VI, and we might expect that m_2 depends not only on B_3 but also on ${}^2a_{nd}$. However ${}^2a_{nd}$ and B_3 are correlated, which is known in terms of the Phillips line [31]. The correlation of ${}^2a_{nd}$ with B_3 is not perfect, showing small deviations from the Phillips line. These arguments are in good accordance with what we observe in Fig. 3, which shows the correlation of m_2 with respect to B_3 with some scatters.

For noble two-body processes, effective range expansion technique often allows us even algebraic relation of the RMEs in terms of ERPs, see, for example, Refs. [32] for the Gamow-Teller matrix element of the $p+p \rightarrow d+e^++\nu$ process. The problem at hand is however too complicate to allow such a mathematical rigor, and we will limit ourselves to an empirical curve fitting. We take the trial function as

$$m_n^{(i)} \simeq \phi_n(B_3^{(i)}) \quad (26)$$

with

$$\phi_n(B_3) = m_n^0 + t_n [(B_3/B_3^{\text{exp}})^\nu - 1], \quad (27)$$

where the superscript i is the model index; that is, $m_n^{(i)}$ ($n = 2, 4$) and $B_3^{(i)}$ stands for the RMEs and 3H BE obtained with the i -th model potential, respectively. Varying the value of ν , values of m_n^0 and t_n are searched by a chi-square fit. The resulting chi-square is found to be parabola shape with minimum at around $\nu = -2.5$. The solution with $\nu = -2.5$ is

$$\begin{aligned} \phi_2(B_3) &= (-21.87 \pm 0.24) - 10.76 [(B_3/B_3^{\text{exp}})^{-2.5} - 1], \\ \phi_4(B_3) &= (12.24 \pm 0.05) + 11.35 [(B_3/B_3^{\text{exp}})^{-2.5} - 1]. \end{aligned} \quad (28)$$

The solution is drawn in solid line in the figure. The above curve fitting procedure turns out to be quite robust. For example, the curves and the values of m_n^0 with $\nu = -1.5$ are almost the same as those with $\nu = -2.5$. Even if we try a simple-minded linear fit, $\nu = 1$, we have $\phi_2(B_3) = -21.73 + 33.65(x_3 - 1)$ and $\phi_4(B_3) = 12.14 - 35.69(x_3 - 1)$, $x_3 \equiv E_{H3}/E_{H3}^{\text{exp}}$. Thus the values of $\phi_n(B_3^{\text{exp}}) = m_n^0$ are quite insensitive to the fitting parameter ν . Furthermore, with the resulting values of $\phi_n(B_3^{\text{exp}}) = m_n^0$, we have $R_c = -0.462 \pm 0.03$ and $\sigma_{nd} = 0.490 \pm 0.008$ mb, which are close to the experimental data. Therefore

one can conclude that the observed strong model-dependence in M1 properties of three-body systems can be traced to the different model predictions of B_3 , and that, once we have correct B_3 , the theory predictions should be very close to the experimental data with little model-dependence.

We have also tried to adjust the nuclear potentials to have correct ERPs. As mentioned, B_3 and ${}^2a_{nd}$ are the relevant ERPs. But since the two ERPs are strongly correlated to each other, simultaneous reproduction of both is rather tricky. This correlation in particular strong due to on-shell NN interaction part, nevertheless three-nucleon interaction can break it. Note that UIX TNI potential consists of two terms. In our calculation, we have readjusted the parameters of those terms to reproduce B_3 and ${}^2a_{nd}$ simultaneously with the Av18 and I-N3LO NN potential. We refer respectively the resulting Hamiltonian as AV18+UIX* and I-N3LO+UIX**. In addition some charge dependence has been added to UIX*, permitting Av18+UIX* to reproduce also ${}^3\text{He}$ binding energy. The corresponding results are given in the bottom lines of the Table VI. The most important observation to be made is that, while the results of Av18, Av18+UIX and I-N3LO differ dramatically, the modified Hamiltonians Av18+UIX* and I-N3LO+UIX** give us almost identical results, which confirms the argument that our theory predictions are model-independent once the ERPs are correctly encoded. The resulting σ_{nd} and R_c are close to the experimental data, but with discrepancy of about two sigmas of the data.

Before closing this section, we would like to make comparison with other calculations for the processes considered in this paper. Viviani et. al. [33, 34] has calculated the M1 properties of $A = 2, 3$ systems with the currents deduced from the adopted nuclear potentials using gauge invariance, adding model-dependent pieces for those part that are not fixed by the gauge symmetry alone. Their results have some variations depending on the adopted potentials [33] and the details of the treatment of the currents. Without model-dependent current part capture cross section is underestimated $\sigma_{nd} = (0.418 \sim 0.462)$ mb, nevertheless one gets $R_c = -(0.429 \sim 0.446)$ quite close to experimental value [34]. Model-dependent currents enable to reproduce experimental cross section, however the photon polarization parameter $R_c = -(0.469)$ becomes larger than the experimental data. Currents related with three-nucleon force further increase capture cross section and photon polarization parameter. A very similar to ours calculation has been recently performed by Pastore et. al. [35], in which electromagnetic current operators have been obtained up-to N³LO within EFT framework.

Δ -isobar as well as pions and nucleons are treated as pertinent degrees of freedom. And they have applied the currents up-to N²LO to $A = 2$ and $A = 3$ systems. To this order, the CT terms – that play a crucial role in removing the model-dependence at short-range physics – do not appear, and they have observed a large cutoff dependence with a substantial under-predictions for σ_{nd} and R_c , $\sigma_{nd} = (0.450 \sim 0.315)$ mb and $R_c = -(0.437 \sim 0.331)$ for the momentum cutoff $\Lambda = (500 \sim 800)$ MeV. We also acknowledge that, using the so-called pionless EFT approach, Sadeghi et. al. [5] have performed up-to N²LO (in their counting scheme) calculation for the σ_{nd} and R_c , achieving a perfect agreement with the data. In their calculations, the np cross section as well as the nd scattering lengths and the binding energies (of $A = 2$ and $A = 3$ systems) are taken as inputs needed to fix their parameters, the magnetic moments have not been considered. Since magnetic moments are sensitive to the D -wave components of the wave functions, it may not be trivial to have accurate theory predictions for the magnetic moments using the pionless EFT. A further study in this issue will be extremely interesting.

IV. DISCUSSIONS

The most natural candidate for the remaining small discrepancy might be the three-body current contributions, which are N⁴LO. It is not difficult to notice that the leading three-body contributions are suppressed for both M1 currents and the nuclear potentials, for exactly the same reason. Furthermore, the soft one-pion-exchange appears as the leading two-body contributions for both of them. Thus we expect that the ratio of the three-body contribution to the two-body contribution is the same order for the M1 RMEs and the nuclear potentials,

$$\frac{\mathcal{M}_{3B}}{\mathcal{M}_{2B}} \sim \frac{\langle V \rangle_{3B}}{\langle V \rangle_{2B}} \sim (0.05 \sim 0.1). \quad (29)$$

Since the TNIs play a crucial role in reproducing the ERPs of three-body systems accurately, we may naively guess that the same will also be true for the relation between three-body currents and the M1 properties. More quantitatively, eq.(29) with Table III tells us that the three-body current contribution will be about $(2 \sim 4)$ % for m_2 and m_4 , which is just the needed size to remove the discrepancy of σ_{nd} and R_c . The same has been demonstrated by Viviani et al. [34], where 3-nucleon currents have let to increase neutron thermal cap-

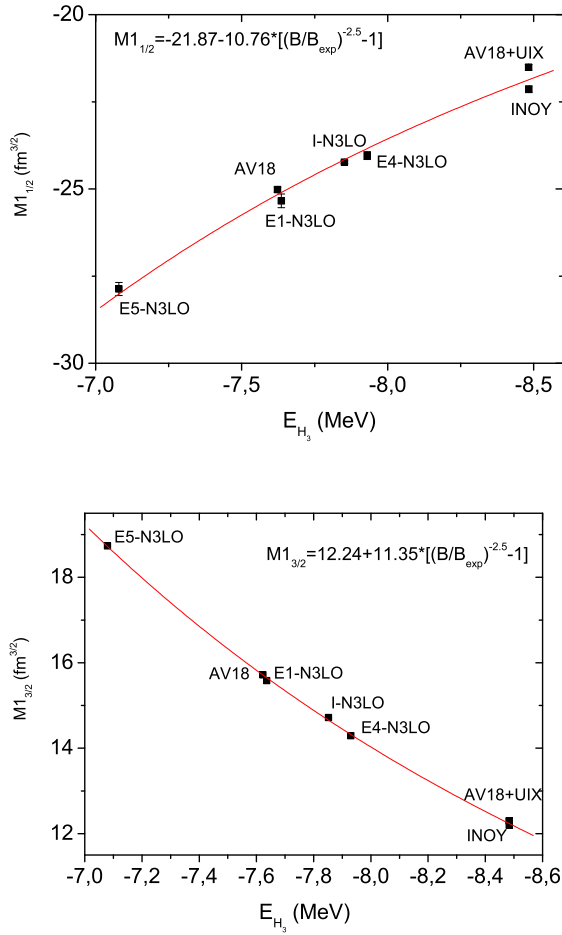


FIG. 3: Radiative capture of thermal neutron by deuteron: correlation of M1 doublet and quartet RME's with triton binding energy.

ture cross section by 0.033 mb. In this regard, taking into account the three-body current contribution – while ignoring other pieces of N⁴LO for simplicity – might be extremely interesting.

V. CONCLUSION

In this paper M1 properties, comprising magnetic moments and radiative capture of thermal neutron observables, are studied in two- and three-nucleon systems. We utilize meson exchange current derived up to N³LO using heavy baryon chiral perturbation theory a la Weinberg. At N3LO, two unknown parameters, g_{4s} and g_{4v} , enter as the coefficients of

contact terms. Following the MEEFT strategy, we have fixed them by imposing the renormalization condition that the magnetic moments of tritium and ^3He are reproduced. Then we analyze the predictions for other M1 properties: magnetic moment of deuteron, as well as observables of the thermal neutron capture on proton and deuteron. Analysis comprise several qualitatively different realistic nuclear Hamiltonians, which allows us to judge on the model dependence of our results. We obtain stable, cut-off independent results, which reconfirms efficiency of MEEFT procedure. Model predictions for two-body observables (deuteron magnetic moment and thermal np capture cross section) scatter closely around the experimentally measured values.

Radiative capture cross section of thermal neutron on deuterons varies a lot from one Hamiltonian to the other. We have demonstrated that this variation is mostly due to the correlation of the capture cross section with a model predicted three-nucleon binding energy. By fixing three-nucleon binding energy to the experimental value one can reduce model dependence below 2% level and obtain model-independent predictions for thermal capture cross section $\sigma_{nd} = 0.490 \pm 0.008$ mb and photon polarization parameter $R_c = -0.462 \pm 0.03$. Within these model-dependent error bars capture cross section agrees with experimentally measured value 0.508 ± 0.015 mb [28]. However photon polarization parameter R_c is obtained slightly too large, like in other studies based on realistic nuclear Hamiltonians and currents [34]. The remaining discrepancy is comparable in size with higher order terms of the EFT, which have been neglected here. We believe that in particular three-nucleon currents, which first appear at N⁴LO in our power counting scheme, should be important.

Acknowledgement

The work of TSP was supported in part by KOSEF Basic Research Program with the grant No. R01-2006-10912-0. The numerical calculations have been performed at IDRIS (CNRS, France). We thank the staff members of the IDRIS computer center for their constant help. TSP is grateful to Prof. Daniel Phillips and Prof. Seung-Woo Hong for valuable discussions. Last but not least we would like to thank Prof. Mannque Rho for his kindness accepting to read the manuscript prior to its publication and giving us important comments.

-
- [1] T.-S. Park, D.-P. Min and M. Rho, Phys. Rev. Lett. **74** (1995)4153-4156; Nucl. Phys. **A596** (1996) 515; T.-S. Park, K. Kubodera, D.-P. Min and M. Rho, Phys. Rev. **C58** (1998) 637.
- [2] T.-S. Park, K. Kubodera, D.-P. Min and M. Rho, Phys. Lett. **B472** (2000) 232.
- [3] C.H. Hyun, T.-S. Park and D.-P. Min, Phys. Lett. **B516** (2001) 321-326.
- [4] J.-W. Chen and M.J. Savage, Phys. Rev. **C60** (1999) 065205; J.-W. Chen, G. Rupak and M.J. Savage, Phys. Lett. **B464** (1999) 1.
- [5] H. Sadeghi and S. Bayegan, Nucl. Phys. **A753** (2005) 291; nucl-th/0610029; H. Sadeghi, S. Bayegan and H.W. Griesshammer, Phys. Lett. **B643** (2006) 263; H. Sadeghi, Phys. Rev. **C75** (2007) 044002.
- [6] R. Skibinski, J. Golak, H. Witala, W. Gloeckle, A. Nogga and E. Epelbaum, Acta Phys. Polon. **B37** (2006) 2905.
- [7] Y.-H. Song, R. Lazauskas and T.-S. Park, Phys. Lett. **B656** (2007) 174.
- [8] T.-S. Park *et al.* , Phys. Rev. **C 67** (2003) 055206; nucl-th/0208055; K. Kubodera and T.-S. Park, Ann. Rev. Nucl. Part. Sci. **54** (2004) 19.
- [9] L.D. Faddeev: Zh. Eksp. Teor. Fiz. **39**, (1960) (Wiley & Sons Inc., 1972). 1459 [Sov. Phys. JETP **12**, (1961) 1014.]
- [10] E. Epelbaum, W. Glöckle, and U.-G. Meissner, Nucl. Phys. **A747** (2005) 362.
- [11] E. Epelbaum, W. Glockle, U.G. Meissner, Nucl. Phys. **A671** (2000) 295.
- [12] J. Carlson and R. Schiavilla, Rev. Mod. Phys. **70** (1998) 743.
- [13] M. Viviani, R. Schiavilla and A. Kievsky, Phys. Rev. **C54** (1996) 534.
- [14] J.L. Friar, B.F. Gibson and G.L. Payne, Phys. Lett. **B251** (1990) 11.
- [15] R.B. Wiringa, V.G.J. Stoks, R. Schiavilla, Phys. Rev. **C51** (1995) 38
- [16] P. Doleschall, I. Borbély, Z. Papp, W. Plessas, Phys. Rev. **C67** (2003) 064005
- [17] P. Doleschall, Phys. Rev. **C77** (2008) 034002.
- [18] D. R. Entem and R. Machleidt, Phys. Rev. **C68** (2003) 041001
- [19] B.S. Pudliner, V.R. Pandharipande, J. Carlson and R.B. Wiringa, Phys. Rev. Lett. **74** (1995) 4396.
- [20] W. Dilg, L. Koester, W. Nistler, Phys. Lett. **36** (1971) 208.
- [21] H. Witala, A. Nogga and al, Phys. Rev. **C68** (2003) 034002.

- [22] A. Nogga, A. Kievsky, H. Kamada, W. Glöckle, L.E. Marcucci, S. Rosati and M. Viviani, Phys. Rev. **C67** (2003) 034004.
- [23] A. Deltuva and A. C. Fonseca, Phys. Rev. **C75** (2007) 014005.
- [24] A. Deltuva, private communication.
- [25] R. Lazauskas and J. Carbonell, Phys. Rev. **C70** (2004) 044002.
- [26] E. Epelbaum, A. Nogga, W. Gloeckle, H. Kamada, U. G. Meissner and H. Witala, Phys. Rev. **C66** (2002) 064001 [arXiv:nucl-th/0208023].
- [27] S. F. Mughabghab, M. Divadeenam, and N. E. Holden, *Neutron Cross Sections from Neutron Resonance Parameters and Thermal Cross Sections* (Academic Press, London, 1981), <http://isotopes.lbl.gov/ngdata/sig.htm>.
- [28] E.T. Journey, P.J. Bendt, and J.C. Browne, Phys. Rev. **C25** (1982) 2810.
- [29] M.W. Konijnenberg et al., Phys. Lett. **B205** (1988) 215.
- [30] S. Pastore, R. Schiavilla and J. L. Goity, arXiv:0809.2555 [nucl-th].
- [31] A.C. Phillips, Nucl. Phys. **A107** (1968) 209.
- [32] T.-S. Park, K. Kubodera, D.-P. Min and M. Rho, Astrophys. J. **507** (1988) 443-453.
- [33] M. Viviani, R. Schiavilla and A. Kievsky, Phys. Rev. **C54** (1996) 534.
- [34] L.E. Marcucci, M. Viviani, R. Schiavilla, A. Kievsky and S. Rosati, Phys. Rev. **C72** (2005) 014001.
- [35] S. Pastore, R. Schiavilla and J.L. Goity, nucl-th/0810.1941.